Bulletin of the Seismological Society of America, Vol. 103, No. 6, pp. 3372–3378, December 2013, doi: 10.1785/0120130117

Ⓔ

Short Note

Lack of Additional Triggered Tectonic Tremor around the Simi Valley and the San Gabriel Mountain in Southern California

by Hongfeng Yang and Zhigang Peng

Abstract We conduct a systematic search of tectonic tremor triggered by distant large earthquakes around the Simi Valley (SV) and the San Gabriel Mountain (SGM) in southern California. Out of 59 large earthquakes between 2000 and 2013, only the 2002 M_w 7.9 Denali fault earthquake triggered clear tremor in the region. The observed travel times of the triggered tremors are consistent with theoretical predictions from tremor sources that are spatially clustered in the SV, close to the rupture zone of the 1994 M_w 6.7 Northridge earthquake. We also estimate the triggering stress threshold as ~12 kPa from measuring the peak ground velocities near the tremor source. The lack of clear tremor beneath the SGM provides a "negative" example for a region where tremor is expected to occur because of clear evidence of fluid-rich zones at the middle crust. The results imply that the necessary conditions for tremor to occur are more than fluid-induced low effective normal stress.

Online Material: Figures of additional tremor inspection, tables of earthquake catalogs, and tremor locations.

Introduction

In the past two decades, tectonic tremor (tremor hereafter) has been observed at a variety of tectonic regions, such as subduction zones and continental strike-slip faults (Peng and Gomberg, 2010; Beroza and Ide, 2011, and references therein). Tremor, sometimes accompanying slow-slip events (SSEs), generally occurs on the fault interface near or below the seismogenic section, coinciding with the transition from unstable to stable sliding (e.g., Rocca *et al.*, 2009; Shelly and Hardebeck, 2010). In addition to occurring spontaneously, tremor can also be triggered by passing seismic waves of regional and teleseismic earthquakes (Peng and Gomberg, 2010, and references therein).

In California, triggered tremors have been extensively observed in the Parkfield–Cholame section of the San Andreas fault (SAF), central California (e.g., Peng *et al.*, 2009; Chao *et al.*, 2013), where ambient tremors are also documented (e.g., Nadeau and Dolenc, 2005; Shelly and Hardebeck, 2010). In stark contrast, observations of tremors triggered by distant earthquakes are rare in northern and southern California, except for the 2002 Denali fault earthquake (Gomberg *et al.*, 2008). A recent systematic search of triggered tremor around the Calaveras fault in north California and the San Jacinto fault (SJF) in southern California has not found additional evidence (Chao, Peng, Fabian, *et al.*, 2012; Wang *et al.*, 2013), except for the triggering along the SJF by the 2011 M_w 9.0 Tohoku-Oki earthquake (Chao *et al.*, 2013). These results suggest either different triggering stress threshold or background noise levels in these regions. Despite these recent studies of tremor, the specific conditions for tremors to occur and their relationship to ordinary earthquakes are still unclear.

Abundant observations of dynamically triggered tremors indicate that effective normal stress at the tremor source regions is low (Peng and Gomberg, 2010). Furthermore, the low effective normal stress is also suggested by the numerical modeling of SSEs on a frictional fault model (Liu and Rice, 2005, 2007). The low effective normal stress is generally a result of the near-lithostatic pore fluid pressure, which has been implied by receiver function studies (Audet *et al.*, 2009) and V_P/V_S ratios (Shelly *et al.*, 2006; Kato *et al.*, 2010). Therefore, it is reasonable to hypothesize that the presence of fluid zones below the seismogenic section of a fault may provide a favorable environment for tremor to occur.

Seismic reflection and refraction studies have identified bright reflective zones in the middle crust beneath the San Gabriel Mountain (SGM) in southern California (Ryberg and Fuis, 1998; Fuis *et al.*, 2001, 2003). Because the reflector amplitude is negative at the top of this zone, it requires the presence of near-lithostatic fluids at such depth (Ryberg and

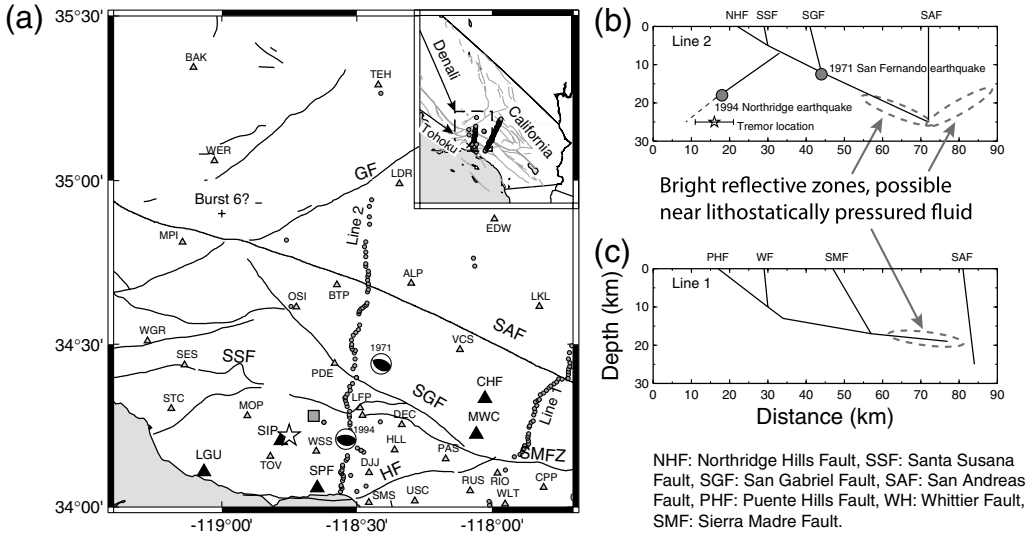

Figure 1. (a) A map of the study region in southern California. The star denotes the average location of tremor bursts 1–5 triggered by the 2002 M_w 7.9 Denali fault earthquake. The cross shows the location of burst 6. The gray square stands for the tremor location from a previous study (Gomberg *et al.*, 2008). The triangles mark seismic stations in the USGS/Caltech Southern California Seismic Network (CI) that we examined in the region. Black triangles represent stations where triggered tremors are observed. Black lines are mapped faults in the region. Gray dots denote the two seismic profiles deployed during the Los Angeles Region Seismic Experiment (LARSE). The inset map shows the location of the study region. Average tremor location (circle) and mapped faults (gray lines), as well as the LARSE lines 1 and 2, are shown. Two arrows show the directions of incoming waves from the 2002 Denali fault and 2011 Tohoku-Oki earthquakes. SAF, San Andreas fault; GF, Garlock fault; SGF, San Gabriel fault; SMFZ, Sierra Madre fault zone; SSF, Santa Susana fault; HF, Hollywood fault. (b) Schematic view of a cross section along the LARSE line 2. Gray dots show locations of two significant earthquakes, the 1971 M_w 6.7 San Fernando and the 1994 M_w 6.7 Northridge earthquakes. The star denotes the tremor location (with 95% confidence interval) determined in this study. Black lines are faults imaged by LARSE results (Fuis *et al.*, 2001, 2003). (c) Similar to panel (b), except for the LARSE line 1 profile.

Fuis, 1998). The fluid zones appear to be associated with the low-angle reverse faults that hosted a series of moderate earthquakes (Fig. 1), for example, the 1971 M_w 6.7 San Fernando and the 1994 M_w 6.7 Northridge earthquakes (Heaton, 1982; Hauksson *et al.*, 1995). In addition to the presence of fluid-rich zones, a master décollement (Fig. 1c) beneath the SGM is interpreted to connect the Puente Hill blind thrust, the Whittier fault, and the Sierra Madre thrust faults (Fuis *et al.*, 2003). Such tectonic setting is similar to that in the Central Range of Taiwan, where triggered tremors have been reported (Peng and Chao, 2008; Chao, Peng, Wu, *et al.*, 2012). Thus, the SGM appears to be a potential spot where tremors are likely to occur. Indeed, Fabian *et al.* (2009) conducted a preliminary study and reported possible tremor signals beneath the SGM triggered by the 2002 Denali fault earthquake. However, it remains unclear whether the tremor observed at the SGM could be explained by the identified tremor source in the neighboring Simi Valley (SV) (Gomberg *et al.*, 2008).

In this study, we conduct a systematic search of triggered tremor around the SGM and the SV in southern California. Our goals are to investigate whether additional events may have triggered tremor in this region and whether the tremors triggered by the Denali fault earthquake share the same source. We first select distant earthquakes that may trigger tremor in the region by estimating the dynamic stresses from their surface-wave magnitudes. We then visually identify tremor signals by examining broadband and filtered seismograms. In addition, we locate the triggered tremors and compare peak ground velocities (PGVs) of all examined earthquakes to determine the triggering stress threshold. Finally, we summarize the triggered tremor activities in the SGM and the SV and discuss the implications of our findings.

Analysis Procedure

The analysis procedure generally follows that of Aiken *et al.* (2013) and is briefly described here. We select earthquakes from the Advanced National Seismic System (ANSS) catalog that have occurred since 2000 and have magnitudes greater than 6. In order to avoid contamination of early aftershocks and effects of static stress, we require event depths to be less than 100 km and their epicentral distances to the broadband station SPF to be larger than 1000 km. We then estimate dynamic stresses generated by these earthquakes using their surface-wave magnitudes (van der Elst and Brodsky, 2010). We only keep events that generated dynamic stresses larger than 1 kPa. Eventually, we find 59 events that met our criteria (Ⓔ Table S1, available in the electronic supplement to this article).

Next, we retrieve eight hours of continuous waveform data, three hours before and five hours after the origin times of these earthquakes, which are recorded at broadband and short-period stations from the USGS/Caltech Southern

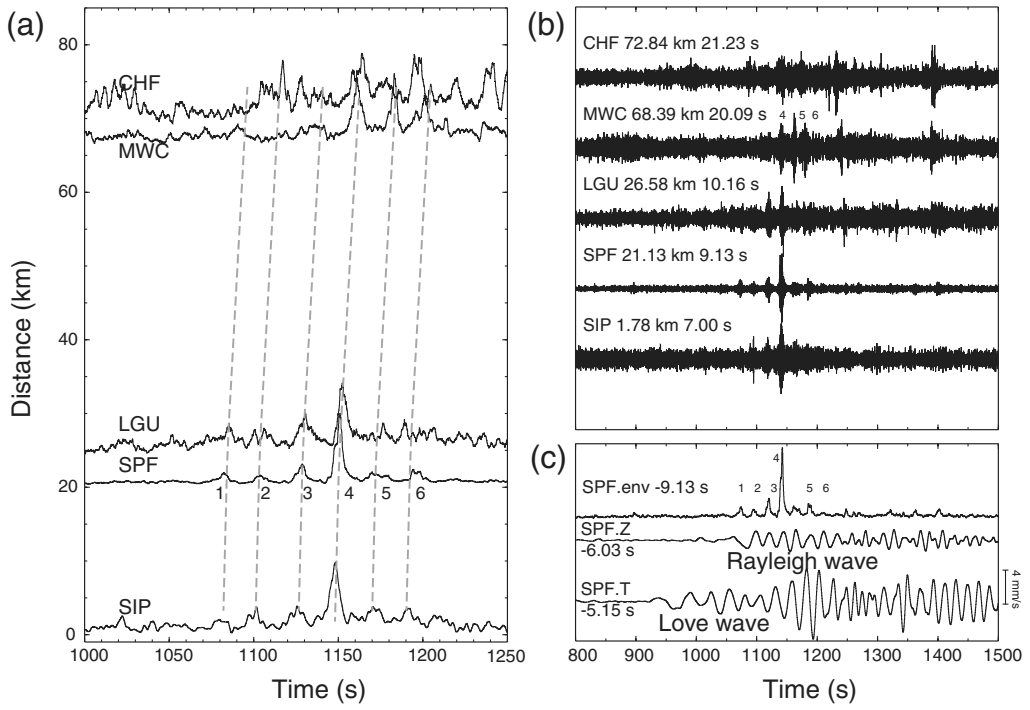

Figure 2. (a) Stacked envelopes of band-pass-filtered (2–8 Hz) velocity seismograms sorted by the epicentral distance to the tremor source located in this study. Dashed line shows predicted arrivals of tremor bursts using the averaged tremor location. (b) Band-pass-filtered (2–8 Hz) velocity seismograms showing tremor triggered by the 2002 Denali fault earthquake. Station names, epicentral distance to the tremor source, and theoretical travel times of tremor are shown on top of each seismogram. All traces are normalized and shifted by the tremor travel times to align the tremor bursts. (c) The stacked envelope function, broadband vertical, and transverse components at station SPF. Broadband seismograms are shifted back to the tremor source using the apparent velocities of Love (4.1 km/s) and Rayleigh waves (3.5 km/s). The stack envelope is normalized and shifted backward by 9.13 s based on the predicted tremor travel times. The exact shifted times are shown by the numbers following the names.

California Seismic Network (CI) around the SGM and the SV (Fig. 1). After removing instrument responses, we inspect the spectrogram to determine a suitable filter band in order to avoid contaminations from regional and teleseismic *P* waves (Peng *et al.*, 2011). In this study, we applied a 2–8 Hz band-pass filter to all waveforms. We then stack the envelopes of filtered three-component velocity seismograms. At certain stations where horizontal components were not available (e.g., station SIP), we only use the vertical component. We then visually inspect the envelopes and band-pass-filtered seismograms to search for tremors triggered by surface waves. Following previous studies (e.g., Peng *et al.*, 2009; Aiken *et al.*, 2013), we identify triggered tremors as nonimpulsive, high-frequency signals that are coherently observed among several stations during surface waves of distant events.

Finally, we locate the triggered tremor bursts by performing a grid search of the minimum residual between theoretical and picked travel times on stacked envelopes (Chao, Peng, Fabian, *et al.*, 2012). We use a 1D velocity model of southern California to calculate theoretical travel times (Shearer *et al.*, 2005). Because the source depth of tremor is not well constrained by this method, we fix the tremor depth to be 25 km, similar to the average tremor depths at the SAF near Parkfield (Shelly and Hardebeck, 2010).

Observations of Triggered Tremor

Similar to the previous study (Gomberg *et al.*, 2008), we observe tremors around the SV triggered by the 2002 M_w 7.9 Denali fault earthquake. A total of six coherent tremor bursts between 1050 and 1250 s have been observed at several stations (Fig. 2a). The most prominent tremor signals are recorded at the broadband station SPF. Similar coherent tremor signals are observed in the time-shifted band-pass-filtered seismograms (Fig. 2b). At stations further distant from the tremor source (e.g. CHF and MWC), only weak tremor signals can be identified on the band-pass-filtered seismograms.

The source of each tremor burst is located separately based on picked arrival times from all possible envelopes (Ⓔ Table S2, available in the electronic supplement to this article). For example, the arrival times of the tremor burst 4 are picked at all five stations (Fig. 2) and the minimum residual is ~3 s, corresponding to a relatively well-constrained location of 34.22° N, −118.80° W (Figs. 1 and Ⓔ S1, available in the electronic supplement to this article). The timings of tremor bursts at stations MWC and CHF appear to match well with the predicted *S*-wave arrivals (Fig. 2a), indicating that one tremor source is sufficient to explain the observations in the SV and the SGM.

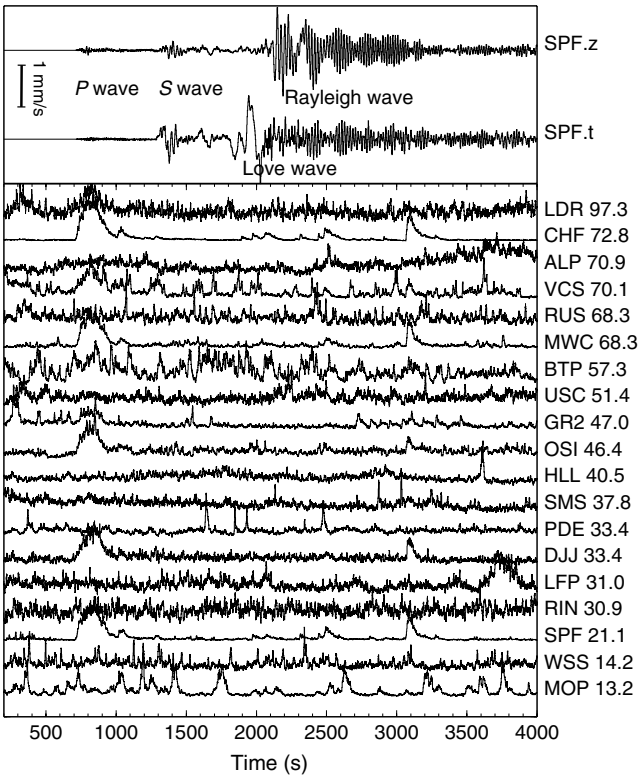

Figure 3. Broadband (upper panel) and stacked envelopes of band-pass-filtered (2–8 Hz) velocity seismograms during the 2011 Tohoku-Oki earthquake. All band-pass-filtered waveforms are normalized individually. Station names and distances in kilometer to the tremor source are marked on right. Zero time is the origin time of the mainshock.

As shown in Figure 1, bursts 1–5 are all located in the SV, close to the tremor location from the previous study (Gomberg *et al.*, 2008) and the epicenter of the 1994 M_w 6.7 Northridge earthquake. Burst 6, however, is located further north near the San Joaquin Valley and Tejon Pass (Fig. 1). To investigate how reliable this location was, we inspect waveforms at nearby stations (Ⓔ Fig. S2, available in the electronic supplement to this article). While tremor bursts are observed at the closest station MPI, the tremor signals are not coherent among stations further south. Instead, the signals at some stations appear to match the travel-time moveout from tremor sources in Cholame (Peng *et al.*, 2008). Hence, we consider burst 6 to be not well constrained.

We also examine the correlations between time-corrected tremor signals and surface waves of the 2002 Denali fault earthquake at station SPF. We calculate the theoretical travel time using an average location from bursts 1–5 and shift the waveforms back to the tremor source (Fig. 2b). We also shift the broadband seismograms using typical values of phase velocities of Love (4.1 km/s) and Rayleigh (3.5 km/s) waves, respectively. The tremor bursts at station SPF appear to initiate when the Rayleigh waves arrived at ~1050 s and correlate with the oscillations of the Rayleigh waves (Fig. 2c).

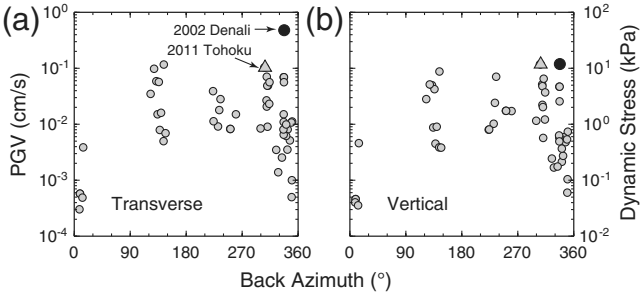

Figure 4. (a) Transverse and (b) vertical peak ground velocities (PGVs) and dynamic stress versus back azimuth of all examined earthquakes recorded at station SPF in the Simi Valley. PGVs are measured on the velocity seismograms after applying a low-pass filter of 1 Hz. Black dot represents triggering earthquake (i.e., 2002 Denali fault earthquake). Gray dots stand for nontriggering events. The 2011 Tohoku-Oki earthquake is shown by the gray triangle.

Besides the 2002 M_w 7.9 Denali fault earthquake, no other examined earthquakes have triggered clear tremor in our study region. For example, the 2011 M_w 9.0 Tohoku-Oki earthquake has triggered widespread tremors around the world, including the Parkfield–Cholame section of the SAF and the Anza section of the SJF (Gonzalez-Huizar *et al.*, 2012; Chao *et al.*, 2013). However, after examining the 2–8 Hz band-pass-filtered envelopes around the SV and the SGM, we did not find any triggered tremor during the surface wave of the Tohoku-Oki mainshock (Fig. 3). Although coherent signals are observed among several stations (e.g., CHF, MWC, and SPF) in the time window of 3000–3500 s (Fig. 3), their relatively low-frequency contents (less than 4 Hz) and nearly identical arrivals indicate that they are likely teleseismic *P* waves of early aftershocks of the 2011 Tohoku-Oki earthquake (Ⓔ Fig. S3, available in the electronic supplement to this article).

Tremor Triggering Threshold and Background Noise

To investigate why the Denali fault mainshock is the only event that triggered tremor in the region, we measure the PGVs of the vertical and transverse components at station SPF for all distant earthquakes (Fig. 4). For those not available at station SPF, we then use the closest station to SPF (Ⓔ Table S1, available in the electronic supplement to this article). On the transverse component, the 2002 Denali fault earthquake generated the largest PGV of 0.48 cm/s, nearly four times larger than that of the 2011 Tohoku-Oki earthquake (0.10 cm/s). In comparison, both earthquakes produced similar PGVs of ~0.14 cm/s on the vertical component. Assuming plane wave propagation, the peak dynamic stress associated with surface waves is proportional to $G\dot{u}/V_S$, in which G is the shear modulus, $\dot{u}$ is ground velocity, and V_S is the phase velocity of the surface wave. Using the typical values of $G = 30$ GPa, $V_S = 4.1$ km/s for Love waves, and $V_S = 3.5$ km/s for Rayleigh waves, we estimate the peak dynamic stress for all examined earthquakes.

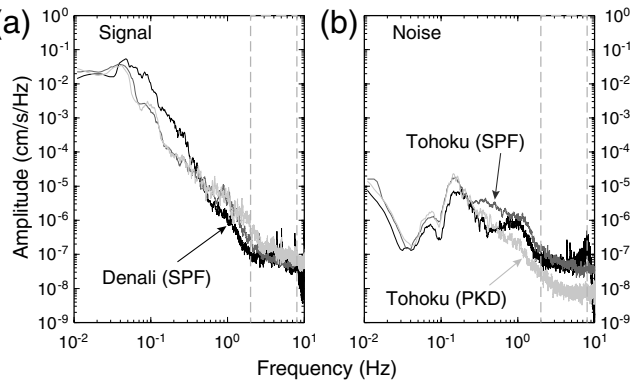

Figure 5. Spectra of (a) signal and (b) noise of velocity seismograms of the 2002 Denali fault (black) and 2011 Tohoku-Oki (gray) earthquakes recorded by the vertical component at station SPF and the 2011 Tohoku-Oki earthquake at station PKD (light gray). Two vertical dashed lines mark the tremor frequency band of 2–8 Hz in this study.

The largest dynamic stress is ~35 kPa, associated with Love waves of the 2002 Denali fault earthquake. The peak dynamic stress associated with Rayleigh waves of the 2002 Denali fault earthquake is ~12 kPa. Hence the apparent triggering threshold is approximately 12 kPa around the SV, higher than the value 2–3 kPa of the SAF near Parkfield, central California (Peng *et al.*, 2009).

To test whether background noise may prevent us from identifying tremors triggered by other earthquakes, we compare both signal and noise of nontriggering events (e.g., 2011 Tohoku-Oki earthquake) with that of the 2002 Denali fault earthquake. The signal spectrum is computed from velocity seismograms during a 600 s time window starting from the initial arrival of Love waves. In the tremor frequency band (2–8 Hz), the spectrum during the Denali fault event is consistently higher than that during the Tohoku-Oki event (Fig. 5a). On the other hand, the noise spectra computed from 600 s window before the *P* arrivals for both earthquakes are somewhat similar, with the Tohoku-Oki noise spectrum having higher amplitudes in 2–4 Hz and lower amplitudes in 4–8 Hz (Fig. 5b). Hence, elevated background noise is not the primary reason why the 2011 Tohoku-Oki earthquake did not trigger tremor in the study region. Furthermore, we also compare the signal and noise levels for the 2011 Tohoku-Oki earthquake at station PKD near Parkfield, central California (Figure 5). Apparently the high-frequency noise level near Parkfield is significantly lower than that in the SV. This could be one of the reasons for the most frequent observations of triggered tremor in the Parkfield–Cholame section of the SAF, as also suggested by Chao, Peng, Fabian, *et al.* (2012).

Discussions

In this study, we conducted a systematic search of triggered tremor around the SV and the SGM in southern California. Our results confirmed the 2002 Denali fault earthquake was the only event that triggered tremor in this region. The triggered tremor was located in the SV, ~20 km west to the 1994 M_w 6.7 Northridge earthquake that occurred on a blind thrust fault dipping ~35° to the south (Hauksson *et al.*, 1995). Although the source depth was not well constrained (set to be 25 km), the triggered tremor likely originated from the same or neighboring fault that generated the 1994 M_w 6.7 Northridge earthquake (Fig. 1). If so, the incoming waves of the 2002 Denali fault earthquake were nearly normal to the strike of this blind low-angle reverse fault, which is a favorable condition for Rayleigh-wave triggering (Hill, 2012). Indeed, we observed the triggered tremor was mainly associated with the Rayleigh waves of the 2002 Denali fault earthquake (Fig. 2c). In addition, we did not observe tremors in the SV and the SGM excited by Love waves and body waves that had been reported elsewhere (e.g., Rubinstein *et al.*, 2007; Ghosh *et al.*, 2009; Peng *et al.*, 2009). Furthermore, the Rayleigh-triggering potential significantly decreases as the incidence angle becomes strike parallel (Hill, 2012). This is also qualitatively consistent with the fact that we did not observe tremor triggered by the 2011 Tohoku-Oki earthquake, although its vertical PGV is similar to that of the 2002 Denali fault earthquake (Fig. 4).

In general, the tremor triggering potential appears to vary with regions and is associated with amplitude, dominant period, and incidence angle of passing waves, as well as the orientation of the fault strike and background tremor activities (e.g., Peng *et al.*, 2009; Rubinstein *et al.*, 2009; Hill, 2012; Aiken *et al.*, 2013; Chao *et al.*, 2013; Wang *et al.*, 2013). Based on the estimation of PGVs of all earthquakes examined in this study, we inferred the apparent triggering threshold in the SV is at least ~12 kPa, much higher than the threshold estimated for the Parkfield–Cholame section of the SAF (2–3 kPa). However, this value is close to that of the SJF near Anza, where a triggering threshold is suggested to be at least 17 kPa (Wang *et al.*, 2013). In our study region, the tremor likely occurred on or near a low-angle reverse fault that ruptured during the 1994 Northridge earthquake. In contrast, the SJF is a nearly vertical right-lateral strike-slip fault that has well-developed damage zones along strike, at least in the top few kilometers of the crust (Yang and Zhu, 2010). Hence, the role of local fault structure on the triggering stress threshold is not well understood yet.

It has been suggested that triggered tremor might just be ambient tremor that is promoted to occur due to loading from passing seismic waves. This is also known as the "clock-advance" model (Gomberg, 2010). Observations of triggered tremor in the Parkfield–Cholame section of the SAF and Taiwan are statistically consistent with this model prediction (Chao, Peng, Fabian, *et al.*, 2012; Chao, Peng, Wu, *et al.* 2012), in which the triggering probability is proportional to the product of ambient tremor rate and the efficacy of triggering waves. In our study region, ambient tremor has not been documented before. Only the 2002 Denali fault earthquake associated with the largest PGV has triggered tremor in the SV. This is consistent with the clock-advance model that in a region with low ambient tremor rate, the peak amplitude

of the triggering waves must be sufficiently large to trigger tremors. However, the absence of additional triggering cases in the region does not allow us to further validate this model.

Our results showed that the tremor signals observed at stations MWC and CHF in the SGM matched the predicted arrivals time from the tremor sources in SV triggered by the 2002 Denali fault earthquake (Fig. 2). However, we note bursts 4 and 5 at station MWC have similar amplitudes, while burst 4 at station SPF in the SV has much higher amplitude than burst 5 (Fig. 2a). It is hence possible that either we mismatched the bursts in these two regions or a second tremor source closer to the SGM is present. If the burst 5 at station MWC was from the same source of the burst 4 at station SPF, the tremor source with the newly picked arrivals is then located at latitude 33.23° N and longitude −118.84° W (Ⓔ Fig. S1b, available in the electronic supplement to this article). However, the minimum travel-time residual for this location is ∼33 s, about one order of magnitude larger than that of the optimal location using the travel time of the earlier burst at station MWC (Ⓔ Fig. S1a, available in the electronic supplement to this article). Furthermore, the predicted travel time from the new location still matches better with the burst 4 at MWC (Ⓔ Fig. S4, available in the electronic supplement to this article). Therefore, we exclude the possibility that the tremor bursts were incorrectly picked between stations in the SGM and the SV.

Although we cannot completely rule out the possibility of a second source beneath the SGM if its travel times coincide with the predicted arrivals from the SV source, the predicted travel times from the source in the SV appear to sufficiently explain all picked arrivals (Fig. 2a). To search for additional evidence of a possible source beneath the SGM, we have examined all available stations in the surrounding regions (Ⓔ Fig. S5, available in the electronic supplement to this article). Unfortunately, only stations MWC and CHF have showed tremor signals that are modulated by the surface waves of the 2002 Denali fault event. Hence, the likelihood of a second tremor source beneath the SGM is very small.

Nevertheless, we have not found any additional evidence of triggered tremor in the SV and the SGM. As mentioned before, the SGM is a region where one would expect to observe tremor based on the presence of near-lithostatic fluid zones in the middle crust and similar tectonic environment to the Central Range in Taiwan, where both triggered and ambient tremors have been observed (Peng and Chao, 2008; Chao, Peng, Wu, *et al.*, 2012). The lack of clear tremor triggering around the SGM indicates that the necessary conditions for tremor to occur are more than the fluid-induced low effective normal stress. Possible candidates include rock type, temperatures, accumulated tectonic stresses, or other conditions not mentioned above. Further observational and numerical investigations of tremor triggering are needed to advance our understanding of tremor source physics and their relationship to ordinary earthquakes.

Data and Resources

Seismograms used in this study were downloaded from the Southern California Earthquake Data Center (http://www.data.scec.org/, last accessed May 2013).

Acknowledgments

This manuscript benefited from valuable discussions and comments from Chastity Aiken, Kevin Chao, and Chunquan Wu. We thank Hector Gonzalez-Huizar, Associate Editor Haijiang Zhang, and an anonymous reviewer for their constructive comments that improved the manuscript. This work is supported by the National Science Foundation CAREER award EAR-0956051 and Southern California Earthquake Center (SCEC). SCEC is funded by NSF Cooperative Agreement EAR-0106924 and U.S. Geological Survey Cooperative Agreement 02HQAG0008. The SCEC contribution number for this paper is 1813.

References

Aiken, C., Z. Peng, and K. Chao (2013). Tremors along the Queen Charlotte Margin triggered by large teleseismic earthquakes, *Geophys. Res. Lett.* **40,** 829–834, doi: 10.1002/grl.50220.

Audet, P., M. G. Bostock, N. I. Christensen, and S. M. Peacock (2009). Seismic evidence for overpressured subducted oceanic crust and megathrust fault sealing, *Nature* **457,** 76–78.

Beroza, G. C., and S. Ide (2011). Slow earthquakes and nonvolcanic tremor, *Annu. Rev. Earth Planet. Sci.* **39,** 271–296, doi: 10.1146/annurev-earth-040809-152531.

Chao, K., Z. Peng, A. Fabian, and L. Ojha (2012). Comparisons of triggered tremor in California, *Bull. Seismol. Soc. Am.* **102,** no. 2, 900–908, doi: 10.1785/0120110151.

Chao, K., Z. Peng, H. Gonzalez-Huizar, C. Aiken, B. Enescu, H. Kao, A. A. Velasco, K. Obara, and T. Matsuzawa (2013). A global search for triggering tremor following the 2011 M_w 9.0 Tohoku earthquake, *Bull. Seismol. Soc. Am.* **103,** no. 2b, 1551–1570, doi: 10.1785/0120120171.

Chao, K., Z. Peng, C. Wu, C. C. Tang, and C. H. Lin (2012), Remote triggering of non-volcanic tremor around Taiwan, *Geophys. J. Int.* **188,** no. 1, 301–324, doi: 10.1111/j.1365-246X.2011.05261.x.

Fabian, A., L. Ojha, Z. Peng, and K. Chao (2009), Systematic search of remotely triggered tremor in northern and southern California, *Eos Trans. AGU* **90,** no. 52.

Fuis, G. S., R. W. Clayton, P. M. Davis, T. Ryberg, W. J. Lutter, D. A. Okaya, E. Hauksson, C. Prodehl, J. M. Murphy, M. L. Benthien, S. A. Baher, M. D. Kohler, K. Thygesen, G. Simila, and G. R. Keller (2003). Fault systems of the 1971 San Fernando and 1994 Northridge earthquakes, southern California: Relocated aftershocks and seismic images from LARSE II, *Geology* **31,** 171–174, doi: 10.1130/0091-7613(2003)031<0171:FSOTSF>2.0.CO;2.

Fuis, G. S., T. Ryberg, N. J. Godfrey, D. A. Okaya, and J. M. Murphy (2001). Crustal structure and tectonics from the Los Angeles basin to the Mojave Desert, southern California, *Geology* **29,** 15–18, doi: 10.1130/0091-7613(2001)029<0015:CSATFT>2.0.CO;2.

Ghosh, A., J. E. Vidale, Z. Peng, K. C. Creager, and H. Houston (2009). Complex nonvolcanic tremor near Parkfield, California, triggered by the great 2004 Sumatra earthquake, *J. Geophys. Res.* **114,** no. B00A15, doi: 10.1029/2008JB006062.

Gomberg, J. (2010). Lessons from (triggered) tremor, *J. Geophys. Res.* **115,** no. B10302, doi: 10.1029/2009JB007011.

Gomberg, J., J. L. Rubinstein, Z. Peng, K. C. Creager, and J. E. Vidale (2008). Widespread triggering of non-volcanic tremor in California, *Science* **319,** 173.

Gonzalez-Huizar, H., A. A. Velasco, Z. Peng, and R. R. Castro (2012). Remote triggered seismicity caused by the 2011, *M* 9.0 Tohoku-Oki, Japan earthquake, *Geophys. Res. Lett.* **39,** L10302, doi: 10.1029/2012GL051015.

Hauksson, E., L. M. Jones, and K. Hutton (1995). The 1994 Northridge earthquake sequence in California: Seismological and tectonic aspects, *J. Geophys. Res.* **100,** no. B7, 12,335–12,355.

Heaton, T. H. (1982). The 1971 San Fernando earthquake: A double event? *Bull. Seismol. Soc. Am.* **72,** no. 6, 2037–2062.

Hill, D. P. (2012). Surface-wave potential for triggering tectonic (nonvolcanic) tremor—Corrected, *Bull. Seismol. Soc. Am.* **102,** no. 6, 2337–2355.

Kato, A., T. Iidaka, R. Ikuta, Y. Yoshida, K. Katsumata, T. Iwasaki, S. Sakai, C. Thurber, N. Tsumura, K. Yamaoka, T. Watanabe, T. Kunitomo, F. Yamazaki, M. Okubo, S. Suzuki, and N. Hirata (2010). Variations of fluid pressure within the subducting oceanic crust and slow earthquakes, *Geophys. Res. Lett.* **37,** no. L14310, doi: 10.1029/2010GL043723.

Liu, Y., and J. R. Rice (2005). Aseismic slip transients emerge spontaneously in three-dimensional rate and state modeling of subduction earthquake sequences, *J. Geophys. Res.* **110,** no. B08307, doi: 10.1029/2004JB003424.

Liu, Y., and J. R. Rice (2007). Spontaneous and triggered aseismic deformation transients in a subduction fault model, *J. Geophys. Res.* **112,** no. B09404, doi: 10.1029/2007JB004930.

Nadeau, R. M., and D. Dolenc (2005). Nonvolcanic tremor deep beneath the San Andreas fault, *Science* **307,** 389.

Peng, Z., and K. Chao (2008). Non-volcanic tremor beneath the Central Range in Taiwan triggered by the 2001 M_w 7.8 Kunlun earthquake, *Geophys. J. Int.* **175,** no. 2, 825–829, doi: 10.1111/j.1365-246X.2008.03886.x.

Peng, Z., and J. Gomberg (2010). An integrated perspective of the continuum between earthquakes and slow-slip phenomena, *Nature Geosci.* **3,** 599–607, doi: 10.1038/ngeo940.

Peng, Z., L. T. Long, and P. Zhao (2011). The relevance of high-frequency analysis artifacts to remote triggering, *Seismol. Res. Lett.* **82,** no. 5, 654–660, doi: 10.1785/gssrl.82.5.654.

Peng, Z., J. E. Vidale, K. C. Creager, J. L. Rubinstein, J. Gomberg, and P. Bodin (2008). Strong tremor near Parkfield, CA excited by the 2002 Denali Fault earthquake, *Geophys. Res. Lett.* **35,** no. L23305, doi: 10.1029/2008GL036080.

Peng, Z., J. E. Vidale, A. G. Wech, R. M. Nadeau, and K. C. Creager (2009). Remote triggering of tremor along the San Andreas fault in central California, *J. Geophys. Res.* **114,** no. B00A06, doi: 10.1029/2008JB006049.

Rocca, M. L., K. C. Creager, D. Galluzzo, S. Malone, J. E. Vidale, J. R. Sweet, and G. Wech (2009). Cascadia tremor located near plate interface constrained by *S* minus *P* wave times, *Science* **323,** 620–623.

Rubinstein, J. L., J. Gomberg, J. E. Vidale, A. G. Wech, H. Kao, K. C. Creager, and G. Rogers (2009). Seismic wave triggering of nonvolcanic tremor, episodic tremor and slip, and earthquakes on Vancouver Island, *J. Geophys. Res.* **114,** no. B00A01(22), doi: 10.1029/2008JB005875.

Rubinstein, J. L., J. E. Vidale, J. Gomberg, P. Bodin, K. C. Creager, and S. D. Malone (2007). Non-volcanic tremor driven by large transient shear stresses, *Nature* **448,** 579–582, doi: 10.1038/nature06017.

Ryberg, T., and G. S. Fuis (1998). The San Gabriel Mountains bright reflective zone: Possible evidence of young mid-crustal thrust faulting in southern California, *Tectonophysics* **286,** 31–46.

Shearer, P., E. Hauksson, and G. Lin (2005). Southern California hypocenter relocation with waveform cross-correlation, Part 2: Results using source-specific station terms and cluster analysis, *Bull. Seismol. Soc. Am.* **95,** no. 3, 904–915, doi: 10.1785/0120040168.

Shelly, D. R., and J. L. Hardebeck (2010). Precise tremor source locations and amplitude variations along the lower-crustal central San Andreas fault, *Geophys. Res. Lett.* **37,** no. L14301, doi: 10.1029/2010GL043672.

Shelly, D. R., G. C. Beroza, S. Ide, and S. Nakamula (2006). Low-frequency earthquakes in Shikoku, Japan, and their relationship to episodic tremor and slip, *Nature* **442,** 188–191.

van der Elst, N. J., and E. E. Brodsky (2010). Connecting near-field and far-field earthquake triggering to dynamic strain, *J. Geophys. Res.* **115,** no. B07311, doi: 10.1029/2009JB006681.

Wang, T.-H., E. S. Cochran, D. Agnew, and D. D. Oglesby (2013). Infrequent triggering of tremor along the San Jacinto fault near Anza, California, *Bull. Seismol. Soc. Am.* **103,** no. 4, doi: 10.1785/0120120284.

Yang, H., and L. Zhu (2010). Shallow low-velocity zone of the San Jacinto fault from local earthquake waveform modeling, *Geophys. J. Int.* **183,** no. 1, 421–432, doi: 10.1111/j.1365-246X.2010.04744.x.

School of Earth and Atmospheric Sciences
Georgia Institute of Technology
Atlanta, Georgia 30332

Manuscript received 9 May 2013;
Published Online 12 November 2013